

ARIVAZHAGAN, A. 2020. Toolpath algorithm for free form irregular contoured walls/surfaces with internal deflecting connections. *Materials today: proceedings* [online], 22(4), pages 3037-3047. Available from:

<https://doi.org/10.1016/j.matpr.2020.03.439>

Originally presented at the 2nd International materials, manufacturing and modelling conference 2019 (ICMMM 2019), 29-31 March 2019, Vellore, India.

Toolpath algorithm for free form irregular contoured walls/surfaces with internal deflecting connections.

ARIVAZHAGAN, A.

2020



Toolpath algorithm for free form irregular contoured walls / surfaces with internal deflecting connections

Arivazhagan.A^{(1,2 a)*}

¹Department, of Mechanical Engineering, High Temperature Research Centre (Coventry), University of Birmingham, UK.

²(Previously) Department of Mechanical Engineering, Indian Institute of Information Technology Design & Manufacturing, Kancheepuram, Vandalur-Kelambakkam Road, Chennai- 600127, Tamilnadu, India.

*Corresponding author. Tel.: 00447860816479

E-mail address: Ari.Anbalagan@htrc.bham.ac.uk

Abstract

This paper presents a toolpath generation method to efficiently machine free form irregular contoured walls / surfaces (FIWS) containing internal deflecting connections (IDC's). The toolpath generation method is based on a series of identifications and calculations, where initially a 'Main Computable Zone (MCZ)' in the Machinable Areas (M_a 's) of FIWS is identified based on the Tool track dimensions (T_a). Then the MCZ's are divided into Split Computable Zones (SCZ's) and Split Computable Zones for Internal Connections (SCZI's) which are subsequently sub divided as 'Categorized Computable Zones' (CCZ) with simple- medium-high complexity. The identification of CCZ's is based on the 10 different types of FIWS representations developed for this study. From the CCZ's categorization of complexity, they are further split into smaller 'Machinable Zones (MZ's)' using a 4-step algorithm. In the algorithm, the first step calculates a common plane (CP) to cut the steep areas in the CCZ's where the tool cannot have full access for machining. Once the CP is identified, the second step is to extend it by moving them along the CCZ's and calculate the necessary 'Machinable Zones (MZ's)' in the next stage. This is done by finding the intersection of CP with the FIWS through a point to point / line plane intersection concept. After this step, the MZ's are re-iterated by including the open and closed surface criteria and is analyzed for the IDC's to be combined in the fourth stage. This is achieved by adding up the IDC's with the existing MZ's computed by the algorithm. At every stage, the algorithm considers tool collision avoidance and tool rubbing in the CCZ's and MZ's . This is by an automatic computation based on the height to fixture clearance for safer neck length which avoids collision and rubbings in the final toolpaths. Finally, a combined tool path is generated for all the MZ's and has been verified / tested for a sample part and impeller containing similar shapes using UG NX / STEP –NC software.

Keywords: toolpath; MCZ; SCZ; CCZ; FIWS; STEP-NC

1. Introduction and Literature Review:

Machining of free form irregular walls / surfaces (FIWS) always been a challenge for manufacturing engineers because of the shapes with sharp transition seen in these parts. These shapes are usually seen in the aerospace components such as impellers and blades [1] where they vary in thickness from top to bottom containing complex cross sectional profiles (CSP's) with varying dimensions. The complexity arises significantly when the gap between the FIWS are closer or lesser than 1 mm and containing internal deflecting connections (IDC's) which are similar to splitter blades [1, 2]. These small IDC's are kept in impellers and blades for the same reason as of splitter blades and in addition to maintain a weight balance while rotation. Generally, these components are first casted then milled in a 3/5-axis milling machine owing to the lead-time faced during an industrial production. At many cases, the machining side pose a big challenge as it is requires geometrically precise 3D CAD model and successful toolpaths. In the present

scenario, many tool path strategies are available to handle these shapes, but to deduce the best machining toolpath the complexity of FIWS must be thoroughly analyzed. This will always depend on user's discretion and experience as the machining surfaces selection is subjective based on machining approach as 3 or 5 axis. At many situations, even an experienced user will have to edit the generated toolpaths or the machining surfaces owing to the following reasons (i) rubbing of tool with the surface of the walls leading to tool / workpiece breakage/chipping (Fig. 1 (a)) (ii) uncut / overcut zones in the machining regions (Fig. 1 (b)) (iii) tool neck engagement collision in the workpiece (Fig. 1 (c))and (iv) tool breakage due to plunging, owing to the variation of the walls/surfaces (Fig. 1 (d)).

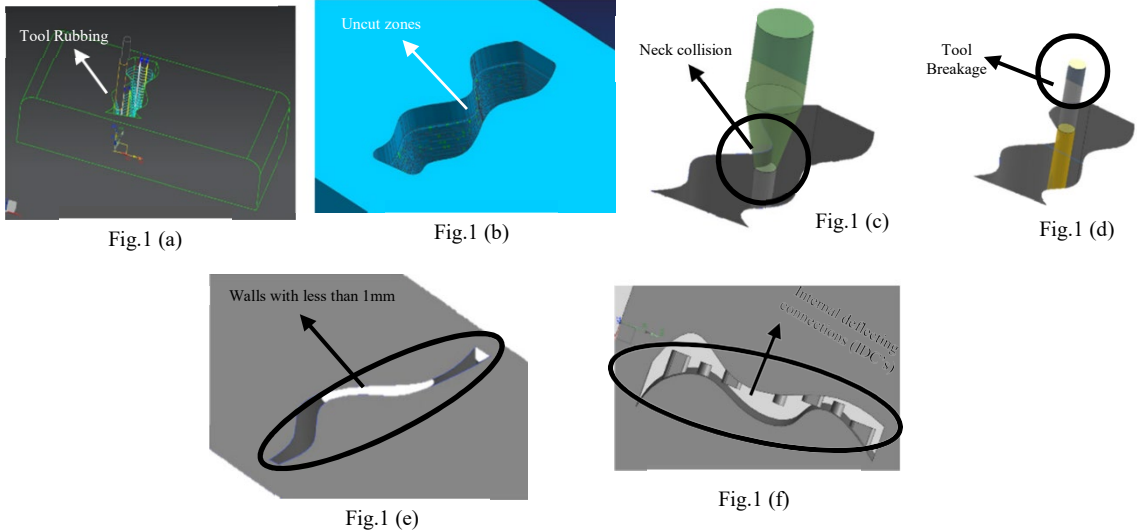


Fig.1 (a) rubbing of tool with the surface of the walls leading to tool / workpiece breakage/chipping; (b) uncut / overcut zones in the machining regions; (c) tool engagement or touch with the neck of the tool in the workpiece and; (d) tool breakage due to plunging like motion owing to the variation of the walls/surfaces (e) gap less than 1-1.5mm; (f) Internal deflecting connections (IDC's) between surfaces/walls

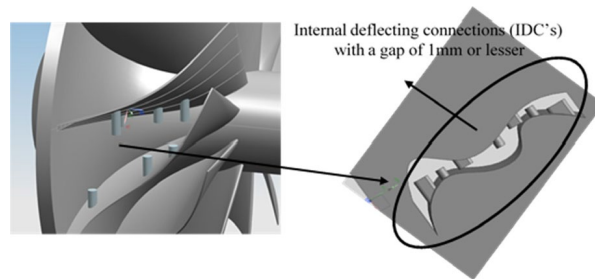


Fig.2 A representation of Internal Deflecting Connections (IDC's) with less than 1mm gap

In any scenario, only two different types of cutting tools have been adopted for machining the FIWS. They are (i) ball nose end mill with a short/long neck and (ii) flat end mill with a short/long neck. As shown in Fig. 1(e) - (f) & Fig. 2 at many instances where the gap between these FIWS are lesser than 1mm, it becomes inevitable for the tool to touch either the walls/surfaces or their internal deflecting connections (IDC's). In order to rectify the problems mentioned above, it is necessary that a successful/robust tool path to be generated where the selection of machinable zones must be computed through a customizable algorithm. As regards, during the past two decades, many researchers [1-14] have handled some of the problems and proposed solutions that occur within the domain of irregular contoured surfaces. But those are focused on a problem that are done for features/walls/surfaces without a minimal gap of 1mm or lesser than that. Moreover, the issues raised in Fig.1 (a-e) are considered separately or in few combinations or not given combined importance for FIWS with a gap of 1mm or lesser. In order to understand the issue faced, it is necessary first to review the research works conducted in the domain. Owing to the vast research conducted in this toolpath generation, articles that are closer to the present work are explained in the forth- coming paragraphs emphasizing the irregular contoured surfaces using 3-5 axis machining.

A concept based on "machining surface" and constant scallop height tool-path generation has been implemented by Tournier & Duc [3]. They suggested that the concept of "machining surface" enables to consider the tool-path as a surface and not only as a set of points or a set of curves. Tool-paths for free form surfaces has been generated by Yin [41]. He presented an approach using progressive fitting and multi-tire solution and used data point models captured by 3D contact or non-contact measuring apparatus. LOD models produced were fitted to different subsets of data points, and he obtained an adaptive rough-cut and finish cut tool-paths. Eungki Lee [5] generated spiral tool path with constant scallop height using contour offset approach. They focused on high speed machining of finish cutting process for sculptured surfaces and developed the tool path by offsetting the boundaries of sculptured surfaces. They also stated that the offset distance is the tool-path interval to maintain the scallop height lesser than the allowed surface roughness. An algorithm to generate tool-paths for clean-up machining in polyhedral objects has been developed by Yongfu Ren et al. [6]. Two steps have been adopted in their work (i) finding the clean-up region between the clean-up boundary points and (ii) generation of clean up tool-paths for the given pathpattern.

A machining strategy for milling a particular set of surface obtained by the technique of cross sectional design is performed by Sotiris & Andreas [7]. First, they considered the surfaces that are formed by sliding the Bezier Curve (Profile curve) along another Bezier Curve (Trajectory). Then tool-paths are generated by offsetting the boundaries of the profile curve matching with the trajectory curve. Stephen [8] developed an integrated form of solution to the problem of optimal tool-path generation for sculptured surface machining using multi axis NC machine. He used the concept of "time-minimal tool-paths" and presented the integral form of the solution to the problem. Avisekh Banerjee et.al [9] proposed an approach to machine floors of pockets using a morphed spiral tool path method. The method adopts biarc and arc spline concept to efficiently generate the tool paths and proved to be efficient with the commercial softwares. Lin Zhiwei et.al [10] proposed a robust 2D point sequence curve approach to efficiently offset tool paths using contour parallel method for pockets with multiple islands. The algorithm consists of three sub-processes (i) islands bridging process (ii) raw offset curve generation and (iii) global invalid loops removal. Finally, they simulated and verified the algorithm with various complex test parts.

Tool paths were generated for a calotte-cutting machine to cut non-planar driving mirrors of complex geometrical shapes by Wings & Juttler [11]. In their work, initially they described the geometry by combining a planar contour with a base surface. Then they generated toolpaths by describing representation of curves and surfaces in a parametric / implicit form. The curves are (i) arc splines (ii) planar splines and (iii) spatial splines. Q. Wang et.al [12] presented an approach to identify the tool orientations for avoiding collisions in five-axis ball-end milling based on two techniques namely (i) Graphics-assisted cubic mapping and (ii) Instantaneous visibility and accessibility cones computation. For each colliding contact location, an accessibility cone is generated from a spherical region instantaneously considering the visibility and occlusion information at that location. The accessibility cone, which conservatively represents the aggregate of all admissible directions of the cutter, is used for measuring the current machining point. Later a collision-free cutter orientation is safely selected from the accessibility cone. Alexandru Dumitrache & Theodor Borangiu [13] presented an approach on generating tool paths based on image IMS10 based depth maps. They adopted a new strategy for machining arbitrary profiles including pockets with islands and validated their algorithm in commercial softwares. Vincent Pateloup et.al [14] presented an approach on 2D curve interpolation for machining pocket using B-Spline approximation. In their work, they first analyzed the existing approximation approaches and used B-Spline approximation for machining the pockets with

smooth corner transition. They concluded that with the proposed algorithm the accuracy is maintained, oscillations are eliminated.

From the literatures it is evident that (i) FIWS machining is conducted without addressing issues faced for features with a minimal gap of 1mm or lesser (ii) FIWS machined in 3/5- axis milling machines does not consider the internal deflecting connections (IDC's) while generating tool paths (iii) There is still a complexity on machining the excess material in between the FIWS features when using smaller diameter with short / long neck cutting tools.

(iv) There is a necessity for most efficient tool path, where the tool spends only a minimum amount of time in air. (v) The tool overall length needs to be kept to the minimum to avoid vibration and to prolong tool life for the most aggressive roughing/finishing operation. (vi) In FIWS machining, focus must be given for integration of tooling, setup and fixturing aspects (vii) The process parameters in a 3/5-axis milling process must be optimized to reduce the machining time and to increase the quality of the product.

Based on the above points, it is decided to proceed with machining of FIWS with internal deflecting connections (IDC's). As a first step, in the next section explains the 10 different types FIWS representations followed by the concept/identification of Main Computable Zones (MCZ's). Then the computation of Split Computable Zones (SCZs) / Split Computable Zones for Internal Connections (SCZIs) is presented with the identification of 'categorized computable zones' (CCZ) based on complexity. After the CCZ calculation, the 4 step algorithm developed for identification of Machinable Zones (MZ's) has been explained. The final section describes the verification and integration of the toolpaths with the UG-NX and STEP-NC with conclusions and scope for future work.

2. Representation and Categorization of free form irregular walls / surfaces (FIWS)

The free form irregular walls / surfaces (FIWS) are formed as a result of either individual or combinations of the primitive representations such as B-Spline and Bezier surfaces. The Machinable Areas (M_a 's) in the FIWS are related to these primitive representations where the cutting tool interacts with the identified M_a 's to remove the material associated with them. Ideally while machining the FIWS, M_a 's are selected by the user and toolpaths are generated. As discussed earlier (Fig.1), in many cases the toolpath generation leads to the problems like rubbings, neck collision, uncut zones and tool breakages. In order to improve the toolpaths and to eliminate these problems, first the FIWS representations must be defined and must be categorized as either simple or complex. In this work, as shown in the Table 1, 10 different types of FIWS representations were defined / developed as simple to complex by analyzing combinations of B-Spline curves/surfaces. These FIWS representations forms the main part of the Main Computable Zones (MCZ's) and helps to identify their complexity for a smoother machining. To develop these 10 different types of FIWS representations, B-spline curve, which is defined by the equation 1, is utilized and a general equation for each is stored to match the MCZ's calculated from the M_a 's. The standard calculation procedure for B- Spline [15] is followed for Single upside Bend SUB-C1 to obtain the equation 3 shown below.

$$C(u) = \sum_{i=0}^n N_{i,k}(u)P_i \quad \text{Eq.(1)}$$

Where, $N_{i,k}$ are B-Spline basis functions of degree k ,

$P_i = \{P_0, P_1, P_2 \dots, P_n\}$ are control points (obtained from geometry) and $U = \{u_0, u_1, u_2 \dots, u_m\}$ is a knot vector.

Where, $m = n + k + 1$; Here $N_{i,k}$ represents the basis function.

$$N_{i,k}(u) = \frac{((u-u_{i-1}) N_{i,k-1}(u)) / (u_{i+k}-u_{i-1}) + ((u_{i+k}-u) N_{i+1,k-1}(u)) / (u_{i+k}-u_{i+1})}{u_{i+k}-u_{i-1}} \quad \text{Eq. (2)}$$











For k (order) =5 and $n=9$, ($n+1$ -control points), and degree = 4 and by considering data points, the standard procedure to calculate B-spline equation [15] is adopted and knot vectors are generated for the same values with the following control points

$$B_0 = (100, 0); B_1 = (196, 34); B_2 = (281, 102); B_3 = (346, 199); B_4 = (383, 321); B_5 = (385, 459); B_6 = (350, 606); B_7 = (274, 751); B_8 = (156, 886); B_9 = (0, 1000)$$

Then based on the Knot vectors for the given data points the final equation is obtained as $C(u) = B_0 N_{0,5}(u) + B_1 N_{1,5}(u) + \dots + B_7 N_{7,5}(u) + B_8 N_{8,5}(u) + B_9 N_{9,5}(u)$ Eq.(3)

In this equation, the B-spline curve is determined using 10 data points and order of five. A total of 15-knot vectors are used to determine the curve equation. Open uniform knot vectors are used in the curve equation. In the same way the equations are calculated for 3D CAD models and converted into surface using a developed subroutine in the UGNX and the values are stored for analyzing the complexity.

Table 1. 10 different types of surfaces considered in the work

S.No	FICS Representation	Name and Complexity Level	S.No	FICS Representation	Name and Complexity Level
1		Single upside Bend SUB-C1	6		Two Closed Bend with Varying end TCBV-C6
2		Double Upside Bend DUB-C2	7		Triple Left Upside Bend TLUB-C7
3		Triple Upside Bend TUB-C3	8		Triple Right Upside Bend TRUB-C8
4		Single Down Bend SDB-C4	9		Triple Round Bend TRB-C9
5		Five Upside Closed Bend FUCB-C5	10		Continuous Multiple Bends CMB-C10

3. Main Computable Zones (MCZ's):

Once the FIWS representations has been defined, the Main Computable Zones (MCZ's) are calculated. These are the areas where the actual machining takes place which are formed as a result of feature specific M_a 's selected by the user. The MCZ's are directly related with the diameter of the cutting tool and the dimensions associated with them. It can be defined as the function of the Tool track dimensions (T_d) and Machinable area (M_a).

$$\text{i.e. MCZ} = F(T_d, M_a) \quad \text{Eq. (4)}$$

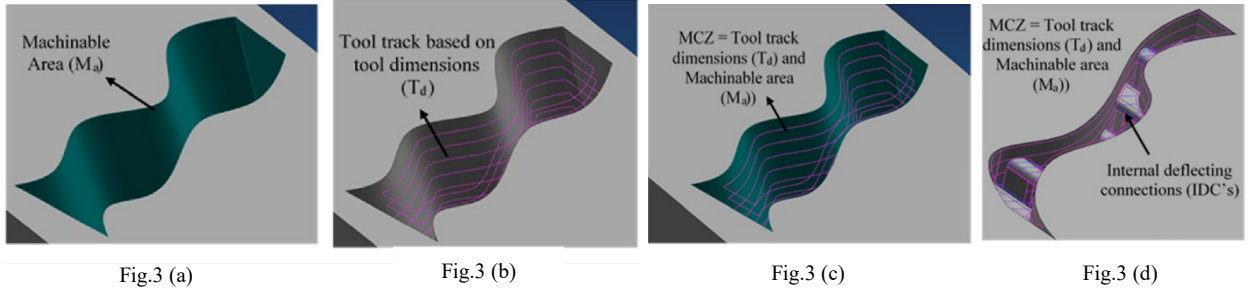


Fig.3 (a) Machinable Area (M_a); (b) Tool track based on tool dimensions (T_d); (c) Main Computable zone (MCZ) showing both M_a and T_d ; (d) Internal Deflecting Connections (IDC's)

Each time, a MCZ is calculated by identifying the total area covered with the M_a 's and by analyzing the radius of the cutting tool. Fig's. 3 (a) to (c) show the relationship between Machinable area (M_a) to the Tool track dimensions (T_d) (in the above case a 3mm (Fig.3 (a)-(c) and 1mm (Fig.3(d) ball end mill is adopted) and the associated MCZ's. Fig.3 (d) is presented for the same concept but for FIWS with IDC's. From the calculated MCZ's, an associated complexity is identified and categorized as 'categorized computable zones' (CCZ) for the further process in the downstream usage. The next section explains how the MCZ's are converted into CCZ's by following the algorithm for the Split Computable Zones (SCZs) / Split Computable Zones for Internal Connections (SCZIs).

4. Computation of Split Computable Zones (SCZs) / Split Computable Zones for Internal Connections (SCZIs)

The next step after calculating MCZ's is to compute the Split Computable Zones (SCZs) / Split Computable Zones for Internal Connections (SCZIs) using a 'Randomized Incremental Algorithm' [15] develop for this purpose. The algorithm considers FIWS and divide the potential MCZ's. As shown in Fig. 4 (a), a localized map MCZ(S) is generated, with sub divided surfaces A to G using subdividing segments Sg1-4. The three lines L1 to L3 in Fig. 4 (b) are the segments starting from the randomized points p1, q1, r1 extending with an end point of p2, q2, r3. The IC1 to

IC4 are the internal deflecting connections (IDC'S) and intersects with the considered map MCZ(S). In order to construct a sub divided the Split Computable Zones (SCZs) / Split Computable Zones for Internal Connections (SCZIs) from the MCZ's first a Data Structure (DS) relationship as shown in the Fig. 4 (c) is developed for the zones covering AB, CD and EFG. It represents the relationship between the subdividing segments Sg1-4, the IDC's and the end points. Based on this, the search is performed for the sub division of splitting zones (as $\Delta_0, \Delta_1, \dots, \Delta_k$) by giving an increment through the lines which are randomly oriented to the FIWS. Then based on the intersections with the MCZ's the SCZs and SCZI's are identified. The following search algorithm has been presented detailing the search procedure adopted to compute the SCZs and SCZI's.

5. Algorithm for SCZs and SCZIs:

Input. A set 'S' of 'n' line segments. (L_1, L_2 and L_3)

Output. The Split Computable Zones (SCZ's) / Split Computable Zones for Internal Connections (SCZI's) with a search structure DS for MCZ(S)

1. Determine a bounding box 'B' so that map MCZ(S) is constructed.
2. Confirm that MCZ(S) contains Line segments L_1, L_2 and L_3 ,
3. Initialize the boundaries to calculate the subdivided segments Sg's.
4. Search for Internal Connection structure IC's inside the subdivided segments Sg. (in our case IC1 to IC4).
5. Compute a random search by considering the surrounding segments around the L_1, L_2 and L_3 of the elements of Sg, between the subdivisions Sg₁ (m_1, n_1, t_1), Sg₂ (m_2, n_2, t_2)Sg_n
6. for $i \leftarrow 1$ to n
7. do \rightarrow Find the set $\Delta_0, \Delta_1, \dots, \Delta_k$ of SCZ's/SCZI's in MCZ intersected by L_i 's (in our case L_1, L_2 and L_3) with the Sg's and IC's (Fig.4(d) and 4(e)).
8. Remove $\Delta_0, \Delta_1, \dots, \Delta_k$ from MCZ and replace them by the new SCZ's/SCZI's that appear because of the insertion of L_i 's (in our case L_1, L_2 and L_3) with Sg's and ICs.
9. Remove the $\Delta_{IC0}, \Delta_{IC1}, \dots, \Delta_{ICk}$ from MCZ's, and create SCZI's.
10. Search / Repeat steps 3-9 for all and categorize the SCZs / SCZIs for further calculations.

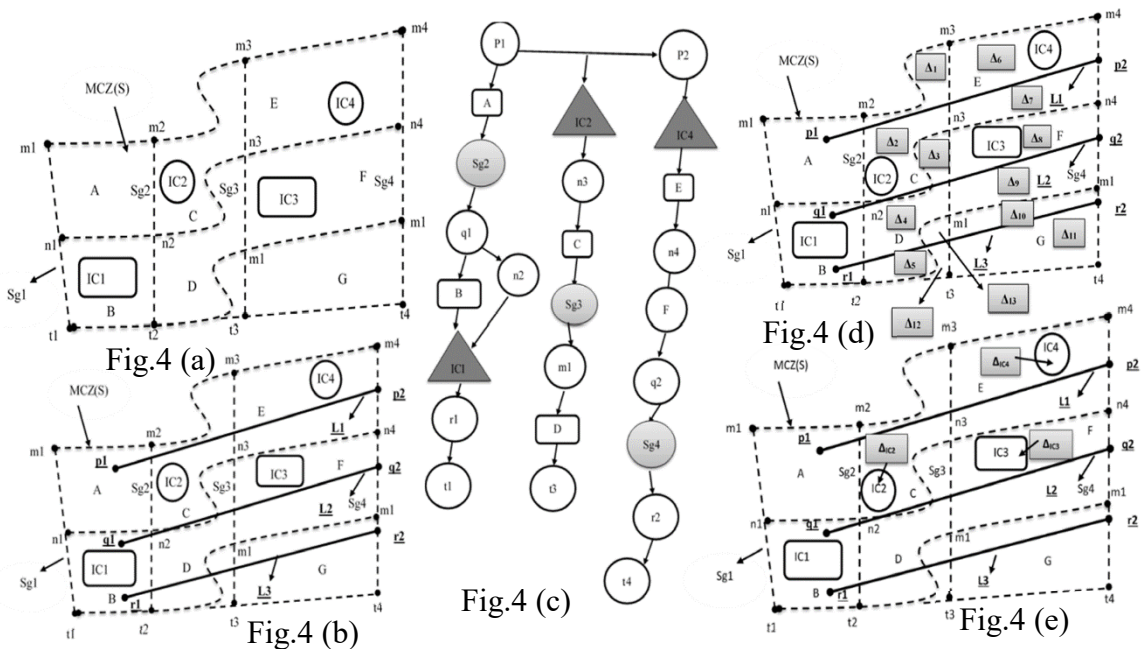


Fig.4. (a)-(b) Representation of localized map MCZ(S); (c) Data Structure (DS) relationship; (d) – (e) sub division of splitting zones based on the randomized incremental algorithm for computation of SCZ's / SCZI's

6. Identification of the ‘categorized computable zones’ (CCZ) based on complexity

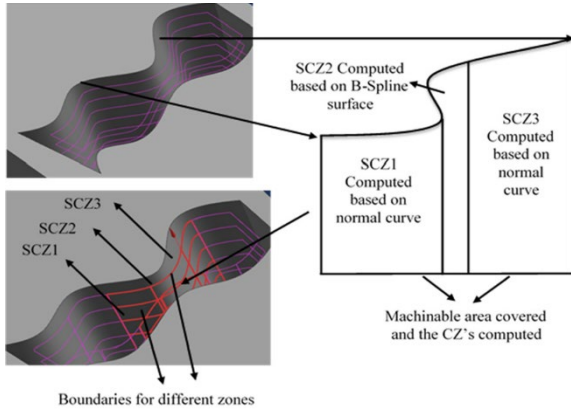


Fig.5(a)

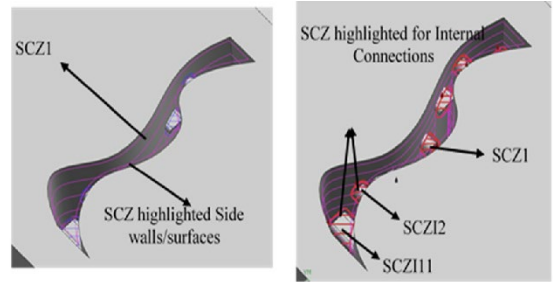


Fig.5 (b)

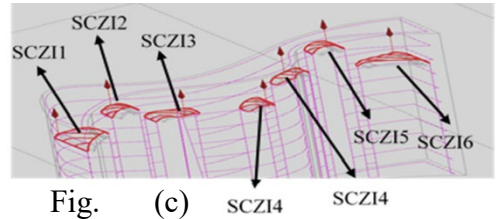


Fig. (c)

Fig.5 (a). SCZ's based on two curved surfaces and one B-Spline surfaces without IDC's; (b) SCZI's for IDC's based on two intersecting curved surfaces and one B-Spline surface; (c) Separated SCZI's with IDC's

Once the process of splitting and identifying the SCZ's / SCZI's is completed, the next stage is to find the order in which these are categorized based on the complexity level as given in Table 1. Fig.5 explains SCZ's and SCZI's calculated for FIWS based on the above algorithm with Fig.5 (b)-(c) and without IDC's Fig.5 (a). The calculated SCZ's/ SCZI's and the ‘categorized computable zones’ (CCZ) identification helps to find the order of machining with the tool access direction of the cutting tool. In the above case (Fig.5), the computation is based on two curved surfaces/intersecting and one B-Spline surface. As given in Table 1, for the part shown in Fig.5, the ‘categorized computable zones’ (CCZ) are identified and tabulated in Table 2 in an increasing order of complexity. Due to page restrictions the full calculation procedure for identification on the complexity is not given. The next sections explains the 4-step algorithm adopted to generate the toolpaths.

Table 2. Categorization of the SCZs based on the complexity level

S.No	SCZ	Name and Complexity Level
1	SCZ1	Double Upside Bend DUB-C2
2	SCZ-11	Single upside Bend SUB-C1
3	SCZ-12	Single upside Bend SUB-C1
4	SCZ-13	Single upside Bend SUB-C1
5	SCZ-14	Single upside Bend SUB-C1
6	SCZ-15	Single upside Bend SUB-C1
7	SCZ-16	Single upside Bend SUB-C1
8	SCZ2	Double Upside Bend DUB-C2

7. 4-step algorithm for the computation of Machinable Zones (MZ's)

7.1 Calculating the common cutting plane to cut the steep areas (CMP's)

In the previous section it is explained, how the SCZ's/ SCZI's are calculated and categorized as CCZ's based on the IDC's in the FIWS. If the toolpaths are generated with the existing SCZ's/ SCZI's then the tool access to the steep areas will not be considered i.e. depth will be ignored. This will result in a tool collision with the neck and the damage to the internal surface of the FIWS. In order to avoid this issue the SCZ's/SCZI's are further split into Machinable Zones (MZ's) by constructing a plane that is closer and either parallel or perpendicular to the surface of the SCZ's/SCZI's.

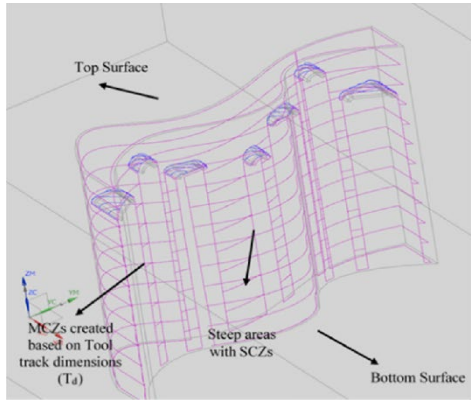


Fig.6 (a)

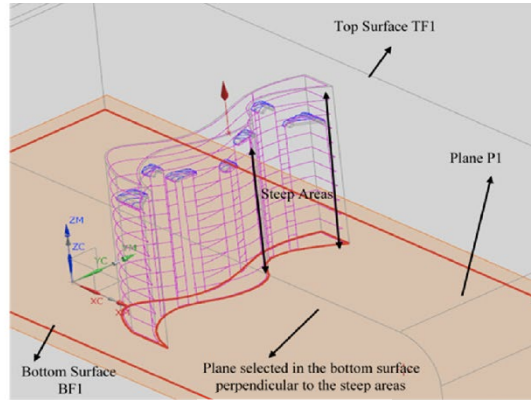


Fig.6 (b)

Fig.6. (a) Representation of the SCZ's/ SCZI's; (b) Selection / Calculation of common plane to cut steep areas

This is done by calculating a closer surface to the opposite side of the (top face) of the tool access direction as shown in Fig.6 (a) and (b). It depicts (Fig. 6(a)) the steep areas where the SCZ's/ SCZI's are calculated but not considering the tool collision avoidance and the tool rubbing. If the same SCZ's/ SCZI's are used then there will be high chance for the tool breakage. Hence, the SCZ's/ SCZI's is divided into separate machinable zones by creating a plane P_1 which is perpendicular (Fig. 6(b)) to the steep areas. The plane is constructed fully to cover the whole part or partially so that all the SCZ's/SCZI's are fully covered.

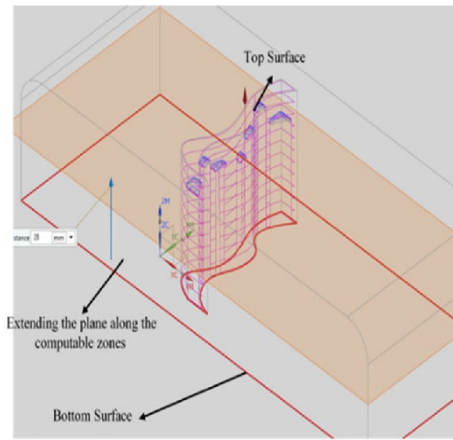


Fig.7 (a)

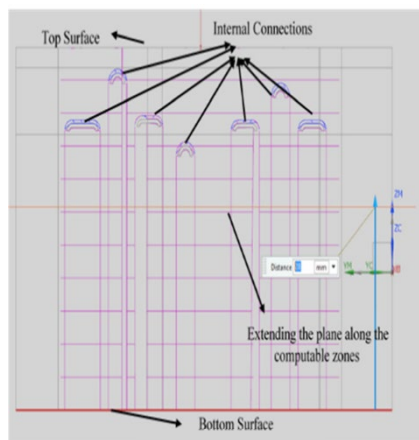


Fig.7 (b)

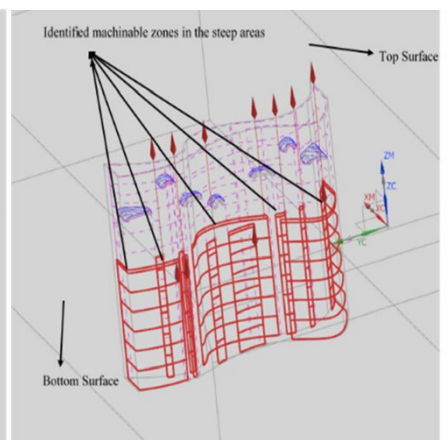


Fig.7 (c)

Fig.7. (a) Finding the common plane; (b) Extending the common plane to cut steep areas; (c) Identification of machinable zones after the intersection of planes with the walls

In the present case, the whole part is covered within the constructed Plane P1. This plane is used to cut the steep areas in one direction and hence may not be used for all other SCZ's/ SCZI's. It should be noted that there can be many cutting planes for a part which is having different SCZ's/ SCZI's. i.e. for each steep area a separate plane must be calculated for subdivision to avoid any tool collision or rubbings that may be faced while machining.

7.2 Extending the common cutting plane by moving them along the split computable zones

Once the common cutting plane is calculated it must be adjusted or moved along the direction of cut to separate the steep areas. This done by either calculating the total tool neck length that is used for the machining of the SCZ's/ SCZI's or by taking the half of the total steep length then comparing it with the neck length of the tool. In both case, the neck of the tool is taken as the reference point for the extension of the cutting plane along the SCZ's/ SCZI's. In the Fig.7 (a) & (b), the cutting plane P1 is moved along the Y direction i.e. the direction that is perpendicular to the steep areas. The movement is adjusted so that all the SCZs are cut into machinable zones which will not have tool collisions or rubbings.

7.3 Identification of machinable zones by finding the intersection of planes with the walls.

The next step is to identify the machinable zones by identifying the intersections of planes with the FIWS. This is done after the plane is extended into the location where the SCZ's/ SCZI's are in possession of cutting them into possible Machinable Zones (MZ's). They are cut into either two or three or multiple based on the connections and interconnectivity between them. In the Fig. 7 (c), it is shown that the identified Machinable Zones (MZ's) in the steep areas are obtained based on the plane location and by calculating the neck length of the tool being used. The top portion of the SCZs are shown as dotted lines and continuous lines for the Machinable Zones (MZ's) separated from them. It also indicates that another plane is required for calculating the machinable areas for other side of SCZ's/ SCZI's and should be done as consecutive operation after this step. For the calculated Machinable Zones (MZ's) the tool access direction or the tool reach is from the top portion on the part.

7.4 Re-iteration of machinable zones by including the open and closed criteria

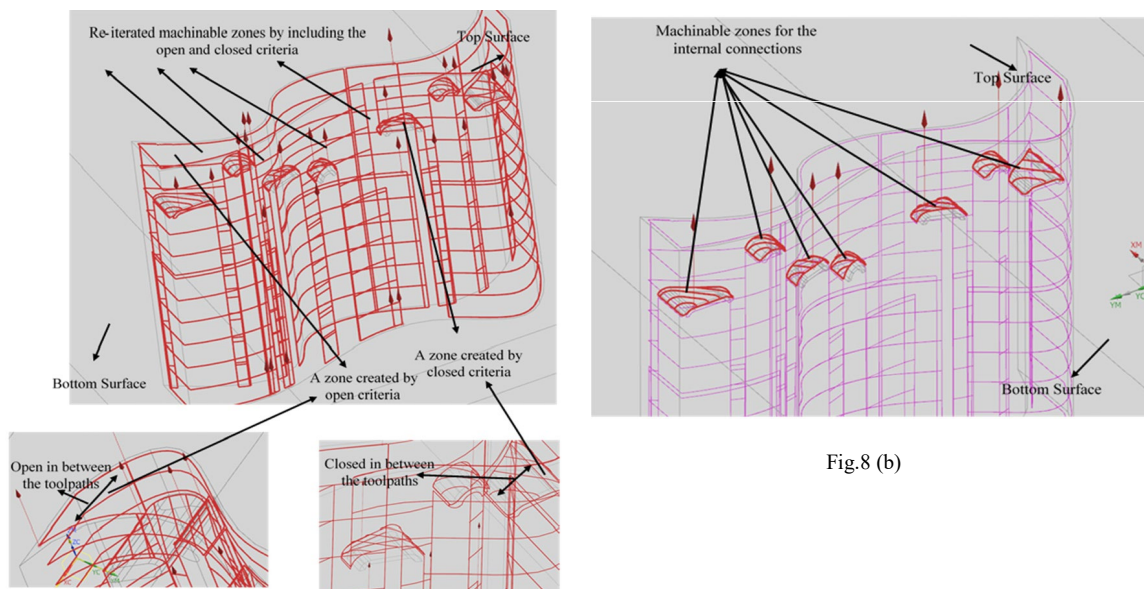


Fig.8 (a)

Fig.8 (b)

Fig.8. (a) Re-iterated machinable zones including open and closed criteria; (b) Re-iterated machinable zones for internal connections including open and closed criteria

Once all the SCZ's/ SCZI's are separated into MZ's from the identified plane, the next step to reiterate the MZs. In this case, the open and closed surface criteria is considered for a particular machinable area that is under the tool reach length. The open and closed criteria is based on the divided surfaces from the planes having either a solid connection between them or a surface connection. The open surface can be defined as a surface that is having continuous movement of tool access in between the parallel toolpaths. The closed surface is usually contains an interconnecting tool paths and hence can be considered as a surface related to solid body. Fig.8 (a) explains the demarcation of the reiterated MZ's by highlighting open and closed surface criteria.

8. Automation and Graphical simulation module of the toolpaths

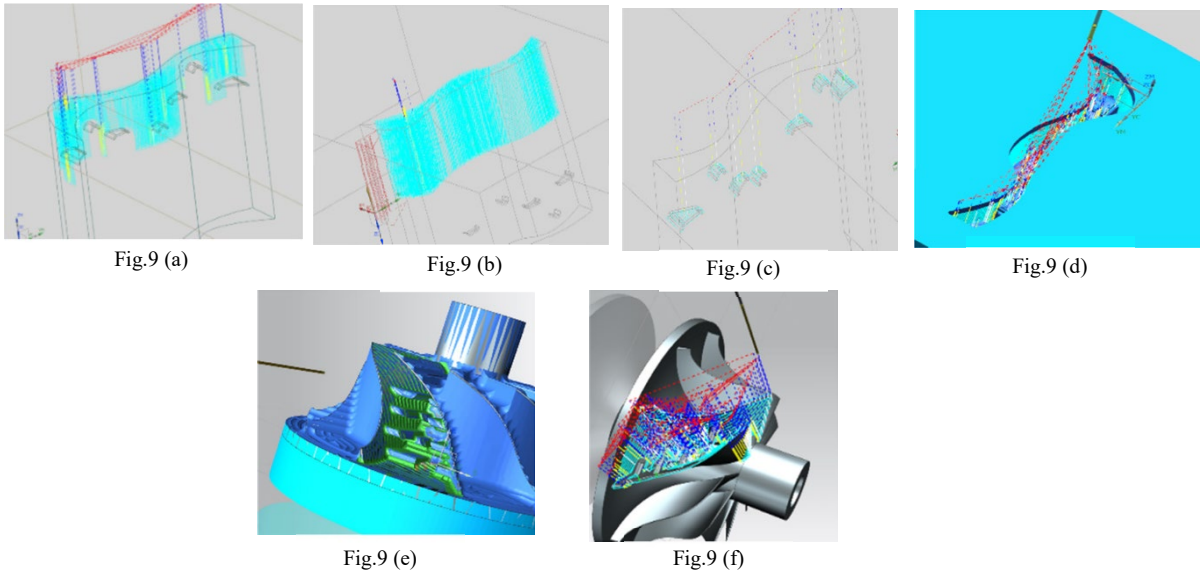


Fig.9 (a)-(f). Final toolpaths generated based on the re-iterated machinable zones including open and closed criteria

Automation is the process of designing and integrating models/toolpaths with/ without the use of graphical environment. Models can be generated using any computer language and an API linked to the CAD package [25]. In this research, UG NX Open API is adopted for automation. NX Open API (User Function) is a collection of routines that allows programs to access and affect the NX Object Model. Based on these routines, the formulated algorithms are coded and verified for its robustness on a test part (Fig.9 (a)-(d)) and an impeller (Fig.9 (e) – (f)). Fig.9 is presented with the final toolpaths integrated with UG/NX and STEP-NC for different sections with the impeller having an IDC's.

9. Conclusions & Scope for future work

The developed algorithm is integrated into UG/NX using NX subroutines and STEP-NC format using STEP-NC Machine software and simulated for a sample part and impeller containing similar shapes. The method proved to be efficient without tool rubbings, neck collision, uncut zones and tool breakages. This work forms a base for the toolpaths with deflecting connections and for subdividing the surfaces which are seen in the FIWS. More improvement is required to handle the shapes that falls under the category of all 10 different types of surfaces as the complexity is increased at each level. At present the toolpath algorithm adopts a 3 axis and partial 5 axis movement at some Machinable Zones. (MZ's). It is planned to proceed with a full 3 to 5 axis implementation for the whole Machinable Zones by further improving the algorithm.

Acknowledgements

The author gratefully acknowledges DST Government of India, for the support to the research on 5 Axis STEP-NC (AP-238) Machining of Free Form / Irregular Contoured Surfaces based on which the present article is contributed.

References

- [1] Ye Yuan, Shouqi Yuan, Analyzing the effects of splitter blade on the performance characteristics for a high-speed centrifugal pump, *Advances in Mechanical Engineering*, 2017; 9(12): 1–11.
- [2] Giovanna Cavazzini, Giorgio Pavesi, Alberto Santolin, Guido Ardizzon and Renzo Lorenzi, Using splitter blades to improve suction performance of centrifugal impeller pumps, *Proceedings of I MechE Part A: Journal of Power and Energy*, 2015, 229(3): 309–323.
- [3] Tournier C, Duc E, A surface-based approach for constant scallop height tool path generation. *International Journal of Advanced Manufacturing Technology*, 2002; 19:318-324.
- [4] Yin Z, Rough and finish tool-path generation for NC machining of freeform surfaces based on a multire-solution method. *Computer Aided Design*. 2004; 36: 1231-1239.
- [5] Eungki Lee, Contour offset approach to spiral tool-path generation with constant scallop height. *Computer Aided Design*, 2003; 35:511-518.
- [6] Yongfu Ren, Hong Tzong Yau, Yuan – Shin Lee, Clean-up tool path generation by contraction tool method for machining complex polyhedral models. *Computer in Industry*, 2004; 54:17-33.
- [7] Sotiris L, Omirou, Andreas C. Nearchou, A CNC machine tool interpolator for surfaces of cross-sectional design. *Rob and Computer Integrated Manufacturing*, 2006; 23:257-264.
- [8] Stephen P. Radzevich, A closed form solution to the problem of optimal tool path generation for sculptured surface machining on multi axis NC machine. *Mathematical and Computer Modelling*, 2006; 43:222-243.
- [9] Avisekh Banerjee, Hsi-Yung Feng, Evgueni V. Bordatchev, Process planning for Floor machining of 2½D pockets based on a morphed spiral tool path pattern, *Computers & Industrial Engineering*, 2012; 63 : 971–979.
- [10] Lin Zhiwei, Fu Jianzhong, He Yong, Gan Wenfeng, A robust 2D point-sequence curve offset algorithm with multiple islands for contour-parallel tool path, *Computer Aided Design*, 2013; 45 :657–670.
- [11] Elmar Wings, Bert Juttler, Generating tool paths on surfaces for numerically controlled calotte cutting system. *Computer Aided Design*, 2004; 36: 325-331.
- [12] Q.-H. Wang, J.-R. Li, H.-Q Gong, Graphics-Assisted Cutter Orientation Correction for Collision-Free Five-Axis Machining. *International Journal of Production Research*, 2007; 45:13: 2875-2894.
- [13] Alexandru Dumitrache, Theodor Borangiu, IMS10-image-based milling toolpaths with tool engagement control for complex geometry, *Engineering Applications of Artificial Intelligence*, 2012; 25: 1161–1172.
- [14] Vincent Pateloup, Emmanuel Duc, Pascal Ray, B-Spline approximation of circle arc and straight line for pocket machining, *Computer Aided Design*, 2010; 42: 817-827.
- [15] Mark de Berg, Otfried Cheong, Marc van Kreveld, Mark Overmars, *Computational Geometry, Algorithms and Applications*, Third Edition, Springer, ISBN 978-3-540-77973-5.